References

1 ARMSTRONG, J.A., BLOEMBERGEN, N., DUCUING, J., and PERSHAN, P.S.: 'Interactions between light waves in a nonlinear dielectric', *Phys. Rev. Lett.*, 1962, **127**, pp. 1918–1939

2 RUSSEL, P.ST.J.: 'All-optical high gain transistor action using second order nonlinearities', *Electron. Lett.*, 1993, **29**, pp. 1228–1229

3 HAGAN, D.J., WANG, Z., STEGEMAN, G., VAN STRYLAND, E.W., SHEIK-BAHAE, M., and ASSANTO, G.: 'Phase-controlled transistor action by cascading of seconed-order nonlinearities in KTP', *Opt. Lett.*, 1994, **19**, (17), pp. 1305–1307

Multiplexed polymer-based chirped grating lenses working at 632.8nm wavelength

R.T. Chen

Indexing terms: Holographic optical elements, Optical polymers

A multiplexed waveguide hologram containing two off-axis chirped grating lenses working at 632.8nm was demonstrated on a glass substrate. Focal lengths of 35 and 37mm were experimentally confirmed. The nature of phase modulation of the holographic medium allows the formation of multiplexed waveguide lenses on the same waveguide emulsion area. The graded index (GRIN) characteristic of the guiding medium allows the formation of polymer-based photonic devices on any substrate of interest which greatly enhances the transferability of polymer-based photonic integrated circuits (PICs) to various optoelectronic circuits.

Successful demonstration of an array of polymer-based photolime gel has recently attracted great interest. In this Letter, we report for the first time the formation of a multiplexed graded index (GRIN, n = 1.4 – 1.6) singlemode polymer waveguide hologram containing two chirped grating lenses on a glass substrate. The physical dimensions of the waveguide lenses are defined by the predesigned mask pattern. The photolime gel used is extracted from animal tissue. When dried, this biophotopolymer is a rigid glass film that shows very little absorption or optical scattering. It is soluble in aqueous solutions and insoluble in most organic solvents such as benzene, acetone, petroleum ether, and absolute alcohol. As a result of this, negative photoresist was used as a masking layer for emulsion sensitisation. The recording of the chirp grating lens can be realised by either using a lithographic tool or holographic recording. In this demonstration, the waveguide lenses were recorded holographically using the geometry suggested in [1].

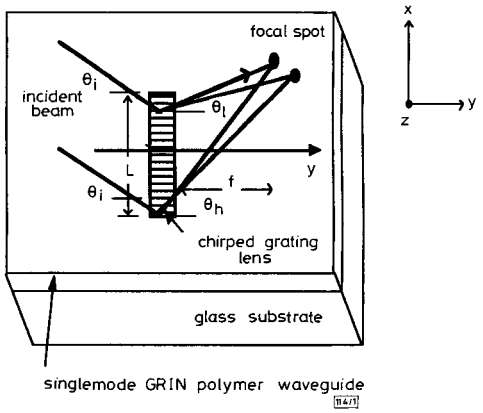

Fig. 1 *Schematic diagram of singlemode graded index polymer waveguide lens on glass substrate*

The nature of phase modulation of the holographic emulsion allows the formation of multiple chirped grating lenses on the same emulsion area. A schematic diagram showing the reconstructed waveguide lenses is shown in Fig. 1. Part of the incident guided beam is diffracted by one of the chirped grating lenses at angles in the range θ_l and θ_h. For the off-axis chirped grating lens shown in Fig. 1, the incident beam cannot be at the Bragg angle across the entire aperture of the lens. It is easy to show that

$$\theta_l = \cot^{-1}\left(\frac{\cos\theta_i}{\sin\theta_i - \frac{\lambda}{\Lambda_l N_{eff}}}\right) \quad (1)$$

and

$$\theta_h = \cot^{-1}\left(\frac{\cos\theta_i}{\sin\theta_i - \frac{\lambda}{\Lambda_h N_{eff}}}\right) \quad (2)$$

where θ_i, θ_l and θ_h are defined in Fig. 1, λ is the optical wavelength, N_{eff} is the effective index of the waveguide mode and $1/\Lambda_l$ and $1/\Lambda_h$ are the grating spatial frequencies of the chirped grating at the indicated locations. Hence, the diffracted beam coming out of the grating region will cross at a distance f, which is defined as the focal length of the chirped grating lens and is determined geometrically. It is clear from eqns. 1 and 2 that the focal length of a guided wave chirped grating lens is controlled by the chirp rate $(1/\Lambda_h - 1/\Lambda_l)/L$ and the effective wavelength, i.e. λ/N_{eff}, within the waveguide. Chirp rates of 680 and 700mm^{-1} are demonstrated for the multiplexed chirped grating lens. Higher chirp rate can be realised by using a fast cylindrical lens for recording. The depth of the phase grating (z-direction of Fig. 1) is equivalent to that of the polymer waveguide. As a result, the diffraction efficiency derived from coupled mode theory is stronger than for a surface relief grating structure with a partial overlap. The formation of a phase grating structure also reduces scattering when compared to a surface-relief structure because of the existence of the surface corrugation caused by etching processes such as chemical etching and ion milling.

Table 1: Design parameters and measured performance of two off-axis chirped grating lenses

	Lens 1	Lens 2
Film index	1.4–1.6 (graded index)	1.4–1.6 (graded index)
Substrate material	Glass	Glass
Waveguide thickness [μm]	10μm	10
Waveguide effective index	1.47	1.47
Chirp rate [mm^{-1}]	680	700
Focal length [mm]	35	37
F#	10.0	10.6
ΔN_{eff}	to 0.1	to 0.1
Diffraction limited spot size (μm) (1/e)	4.2	4.5
Measured 3dB width (μm) (1/e, main lobe)	5.6	6.2
Angular field of view (deg)	6	6
Waveguide propagation loss [dB/cm]	0.1	0.1

The polymeric material we used has a transmission bandwidth from 280 to 2800nm. A polymer-based chirped grating lens working in the UV and visible spectra can thus be realised on high index substrates [2] such as GaAs, Si and $LiNbO_3$. Multiplexed GRIN polymer waveguide lenses working at a wavelength of 632.8nm are shown in Fig. 2 where a guiding layer and two focusing waveguide lenses are clearly shown. The performance features and the design parameters for two waveguide lenses are summarised in Table 1. The range of index tuning is ~1.4 – 1.6. The output end face of the device was further cleaved to facilitate near-field imaging. The diffraction efficiency at λ = 632.8nm was measured to be 32 and 28%, respectively. The linear dimension of the spot size in the depth direction is confined by the waveguide depth, which is 10μm for the reported device shown in Fig. 2.

The wide transmission bandwidth and the GRIN characteristic of the polymer thin film allows the formation of a visible waveguide lens on a lossy high index substrate. The GRIN characteristic allows the formation of a guided wave device transferable to any substrate of interest and the wide transmission bandwidth

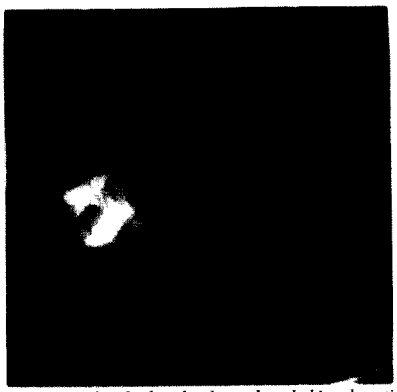

Fig. 2 *Observation of multiplexed polymer-based chirped grating lenses on glass substrate working at 632.8nm*

significantly expands the communication bandwidth of the signal carrier beams. Availability of a waveguide hologram [3] and the integrated transceiver circuitry [4, 5] will greatly enhance the chip-to-chip and module-to-module optoelectronic interconnects using the polymer/III-V material system combination. Furthermore, the large transmission bandwidth of the polymer film (280 – 2800nm) significantly enlarges the optical signal bandwidth for the polymer-based waveguide lens [2].

In summary, we report for the first time the formation of a multiplexed hologram containing two polymer based off-axis chirped grating lens working at a 632.8nm wavelength on a glass substrate. Diffraction-limited spots were also demonstrated. Unlike surface-relief gratings, where grating multiplexibility is not achievable because of their binary nature, the holographic waveguide emulsion we employed is a phase holographic material with an index modulation as high as 0.2. A large number of grating lenses can be multiplexed onto the same area.

Acknowledgment: This research was sponsored by the US Army Research Lab.

14 February 1995
Electronics Letters Online No: 19950635

R.T. Chen (*Microelectronics Research Center, Department of Electrical and Computer Engineering, University of Texas, Austin, TX 78712, USA*)

References

1 KATZIR, A., LIVANOS, A.C., SHELLAN, J.B., and YARIV, A.: 'Chirped gratings in integrated optics', *IEEE J. Quantum Electron.*, 1977, **QE-13**, pp. 296–304

2 CHEN, R.T., PHILLIPS, W., JANNSON, T., and PELKA, D.: 'Integration of holographic optical elements with polymer gelatin waveguides on GaAs, $LiNbO_3$, glass and aluminium', *Opt. Lett.*, 1989, **14**, pp. 892–894

3 CAMPBELL, J.C., KUCHIBHOTLA, R., SRINIVASAN, A., LEI, C., DEPPE, D.G., HE, Y.S., and STREETMAN, B.G.: ''. OSA Topical Meeting on Integrated Photonics Research, 1991, WE5, p. 73

4 FORREST, S.R., TANGONAN, G.L., and JONES, V.: 'A simple 8 × 8 optoelectronic crossbar switch', *J. Lightwave Technol.*, 1989, **LT-7**, pp. 607–614

5 CHEN, R.T.: 'Graded-index polymer-based waveguide lens working at visible wavelengths on GaAs substrate for optoelectronic interconnects', *Appl. Phys. Lett.*, 1993, **62**, pp. 2495–2497

Observation of infrared intersubband emission in optically pumped quantum wells

Z. Moussa, P. Boucaud, F.H. Julien, Y. Lavon, A. Sa'ar, V. Berger, J. Nagle and N. Coron

Indexing terms: Optical pumping, Semiconductor quantum wells, Stimulated emission

Mid-infrared intersubband emission is investigated in GaAs/AlGaAs asymmetric coupled quantum wells exhibiting an energy separation between the ground and first excited subbands close to the LO-phonon energy. The authors show that an infrared emission occurs between excited subbands under intersubband optical pumping.

The large oscillator strengths, combined with a moderate broadening associated with intersubband transitions in semiconductor quantum wells, are favourable properties for optical emission [1, 2]. However, for an intersubband transition in the infrared, the nonradiative scattering processes through LO-phonon emissions lead to extremely short lifetimes of carriers in the excited subbands. Intersubband lasing emission has been recently achieved based on perpendicular transport of electrons in a sophisticated resonant-tunnelling multiquantum well structure [3]. Very recently, an alternative design for achieving mid-infrared intersubband emission has been proposed based on intersubband optical pumping of a three-subband quantum well structure [4]. It was predicted that almost complete population inversion between the two upper subbands can be achieved when the energy separation between the ground and first excited subbands equals the LO-phonon energy.

In this Letter, we investigate this situation in an asymmetric coupled GaAs/AlGaAs quantum well (ACQW) structure designed to meet the above condition. We report the observation of 3-2 intersubband emission at 14μm induced by optical pumping at 9.8μm of the 1-3 intersubband transition. The assignment of the emission is confirmed by Fourier transform infrared (FTIR) spectroscopic measurements.

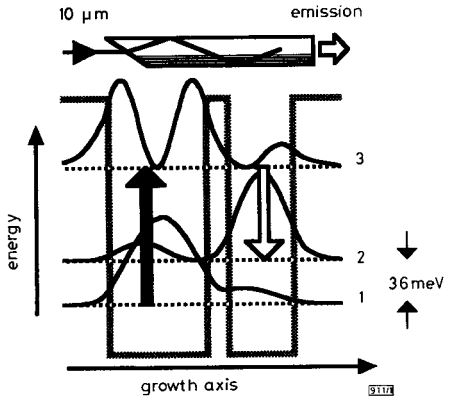

Fig. 1 *Conduction band profile of asymmetric coupled quantum well structure and experimental sample configuration*

The sample containing 100 ACQWs was grown by molecular beam epitaxy on a semi-insulating GaAs substrate. Fig. 1 shows the conduction band profile of the ACQW structure. Each period consists of $Al_{0.22}Ga_{0.78}As$ barriers with GaAs wells. The thicknesses of the wells and intermediate barrier are 7.5, 5 and 1.7nm, respectively. The structure is modulation-doped at the centre of the 20nm $Al_{0.22}Ga_{0.78}As$ barrier separating each period, to provide a sheet electronic concentration of $10^{11}cm^{-2}$ in the wells. The asymmetry of the structure allows direct optical pumping of the 1-3 intersubband transition. The emission is expected between subbands 3 and 2. Envelope wave function calculations including band-bending corrections predict a transition energy at 124, 88 and 36meV for the 1-3, 2-3 and 1-2 intersubband transitions, respectively. As seen, the energy spacing between subbands 2 and 1 is close to the LO-phonon energy in GaAs (36meV). In such a situation, the 2-1 nonradiative relaxation is expected to be faster